

STRAIN MONITORING OF GLASS FIBER EPOXY COMPOSITES USING A REDUCED GRAPHENE OXIDE DEPOSITED INTERPHASE

Haroon Mahmood¹, Massimo Bersani² and Alessandro Pegoretti¹

¹Department of Industrial Engineering, University of Trento, via Sommarive 9, Italy
Email: haroon.mahmood@unitn.it, alessandro.pegoretti@unitn.it

²MiNALab Laboratory, Bruno Kessler Foundation, Via Sommarive 18, 38123 Trento, Italy
Email: massimo.bersani@fbk.eu,

Keywords: Graphene, Interphase, Strain monitoring, Fragmentation test, Electrical conductivity

Abstract

Strain monitoring capabilities of reduced graphene oxide (rGO) coated glass fiber (GF)/epoxy multiscale composites are studied. Using a modified Hummer's method followed by ultrasonication technique, a stable and uniform aqueous dispersion of negatively charged GO was obtained. Electrophoretic deposition (EPD) technique was then applied to deposit GO on GF by placing them in front of a metal anode in the GO bath. At a constant voltage under direct current, a quite uniform deposition of GO nanosheets was obtained on GF. Being insulating in nature, GO was reduced using hydrazine hydrate to partly restore the electrical conductivity of graphene. These hierarchical fibers were aligned within a bicomponent epoxy resin to create unidirectional hybrid GF epoxy composites. The samples were then subjected to various mechanical loading conditions and both longitudinal strain and electrical resistance were monitored simultaneously. The electrical resistance simultaneously changed with the variable applied strain confirming the possibility of graphene coated fibers to be used as strain monitoring sensors in load-bearing components.

1. Introduction

In the present century, much of the attention in the polymer composite research is given towards the integration of nanomaterial to create a new generation of materials with good mechanical properties but also functional properties embedded in the structure. The use of nanomaterials like silica [1], graphene [2] and carbon nanotubes [3] etc. in polymers have demonstrated synergistic effects which marks a wide array of applications of such polymer nanocomposites. In particular, the incorporation of carbon nanomaterials as functional fillers in polymer composites has been of great interest due to the functional groups attached to their surface and also the presence of intrinsic electrical conductivity [4]. This phenomenon has paved the way towards self-sensing or in-situ structural health monitoring of carbon nanomaterial reinforced polymer composites like in case of CNT [5] and graphene [6]. Recent decade has seen an exponential rise of interest in graphene, a superlative nanomaterial, which has demonstrated to be a promising and exciting research area in many fields of science and engineering. Some exceptional noted properties of graphene include high electron mobility, high thermal conductivity and mechanical properties [7, 8]. Hu et al. have recently discussed in detail the use of graphene polymer nanocomposites for structural and functional applications [9]. The focus of this paper is to demonstrate a new way to use rGO as an interphase in fiber reinforced polymer composites for inducing multifunctionality in the structure. With the creation of hierarchical fibers through graphene as an interphase, an improvement in tensile and flexural properties has been reported [10]. However, much of the benefits of graphene's electrical and thermal conductivity features have to be combined and explored in polymer composites. Here we report on the strain-monitoring of GF/epoxy composites in which GF were coated with rGO. The coating was done through electrophoretic deposition on GF under a voltage field. The resulting coated fibers were used to create

multiscale composites with bicomponent epoxy matrix. Various strain monitoring tests were performed to investigate the multifunctional properties of such hierarchical composites.

2. Experimental

2.1. Materials and Methods

Graphite powder, potassium permanganate, sulfuric acid, sodium nitrate and hydrogen peroxide were purchased from Sigma Aldrich while hydrochloric acid was from Codec Chemical Co. Ltd.. E-glass fibers (manufactured by PPG Fiber Glass, trade name: XG 2089) with an average diameter of $16.0 \pm 0.1 \mu\text{m}$. A bicomponent epoxy resin (epoxy base EC 252 and hardener W 241) was provided by Elantas Italia S.r.l. The physical properties of epoxy resin cured at room temperature for 3 h followed by 15 h at 60°C are summarized in Table 1.

Table 1. Physical properties of epoxy resin.

Physical Property	Value
Glass transition temperature (T_g)	28°C
Thermal degradation	340°C
Yield stress (σ_y)	$22.8 \pm 2.4 \text{ MPa}$
Tensile strength (σ_T)	$26.1 \pm 1.1 \text{ MPa}$
Young's Modulus	$795 \pm 28 \text{ MPa}$

GO was synthesized using an approach similar to Hummer's method [11]. The obtained brown solution was dried in a vacuum oven at 50°C for at least 36 hours to obtain GO powder. A schematic description of the EPD process used to deposit GO nanosheets on GFs is depicted in Figure 1. A stable suspension is the key for uniform deposition of graphene on GFs. Initially, GO powder was added in water (concentration: 1 mg/ml) and the solution was subjected to bath-sonication for 1 hour. Two copper plates were used as electrodes in the EPD process. Strands of GFs (fixed on a window frame) were placed near the anode since GO display negative potential due to functionalities attached during the oxidation reaction. Hence, during the EPD process GO migrated towards the anode and deposited on the GFs. EPD was carried out at 10 V/cm with a constant deposition time of 5 min and an electrodes gap of 2 cm. A second EPD cycle was performed under the same conditions while reversing the GFs so that a homogenous deposition could be achieved on the fiber surface. The coated samples were dried in a vacuum oven at 40°C for 12 hours. The dried fibers were treated with the vapors of hydrazine hydrate at 100°C for 24 hours to reduce the GO coated over fibers as reported somewhere else [12]

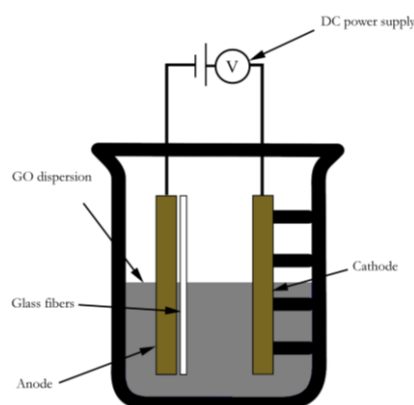


Figure 1. Schematic diagram of electrophoretically coating graphene nanosheets on GF.

Hybrid macrocomposites containing rGO coated GF were created by hand lay-up method. This method consists in placing strands of rGO coated GF in a silicon mold in laminas and subsequently infuse each laminae with epoxy resin. The curing was carried out as mentioned in section 2.1. On the cured specimens (100 mm × 13 mm × 2 mm), a conductive silver paste on the cross section was applied at a mutual distance of 30 mm and thin aluminum sheet was also covered over the silver paste to avoid ohmic resistance of electrical contacts.

2.2. Characterization and Testing

Using X-ray diffraction technique (Rigaku III D-max diffractometer / monochromatic radiation Cu-K α line with $\lambda = 51.54056\text{\AA}$), the oxidation level of graphite, GO and rGO were evaluated. A Nikolet Avatar 330 device with a 4 cm^{-1} resolution was employed to record fourier transform infrared (FTIR) spectra to investigate the functional groups associated with the samples graphite, GO and rGO powders. These were individually mixed with potassium bromide powder to form homogeneous mixtures and thin discs for analysis were made in a compression mold at 10 bar pressure. Elemental composition of GO and rGO was examined by X-ray photoelectron spectroscopy (Kratos Axis Ultra DLD) machine fitted with a monochromatic Al K α (1486.6 eV) x-ray. An emission angle of 90° between the axis of the analyzer and the sample surface was maintained and O 1s and C 1s core lines of each sample were collected. The relative elemental percentage was calculated using the integrated area of the fitted core lines, after Shirley background subtraction, and correcting for the instrument sensitivity factors. Field emission scanning electron microscopy (FESEM) using a Zeiss SUPRA 40 microscope was employed to analyze the morphology and coatings of graphene nanosheets on GF. For electrical characterization, especially to measure resistivity values, two different measurement methods were employed based on the electrical nature of the materials. For specimens having resistivity levels equal to and beyond $10^6\ \Omega\text{-cm}$, the electrical resistivity was measured using a Keithley 8009 resistivity test chamber coupled with a Keithley 6517A high-resistance meter. While for conductive samples, the high resistance meter (Keithley model 6517A) was used.

3. Results and discussion

In figure 2, x-ray diffraction pattern of precursor graphite clearly shows an intense peak (0 0 2) at 26.4° which is typical of pristine graphite powder in crystalline form. An oxidation reaction of graphite powder shifts the (0 0 2) graphite peak to a (0 0 1) diffraction peak of GO which can be seen in the figure 2b. This induces an increase in interlayer spacing of graphite layers because of insertion of oxygen functional groups in GO as well as water molecules hence broadening the peak and lowering of intensity [13]. Finally the rGO diffractogram has the peak relocated back to the original location of pristine graphite due to the removal of most of the oxygen groups from GO and consequently decreasing the interlayer spacing.

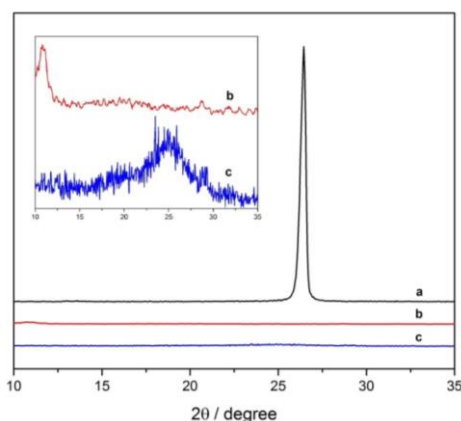


Figure 2. X-ray diffractograms of (a) graphite, (b) GO and (c) rGO. The internal box shows the magnified picture of diffractograms of (b) GO and (c) rGO

Fig. 3 shows that in comparison to pristine graphite, the FTIR spectrum of GO shows relatively intense peaks of functional groups like epoxy C-O, C=O and O-H at wavenumbers approximately 1085 cm^{-1} , 1625 cm^{-1} and 3830 cm^{-1} respectively hence confirming the destruction of original extended conjugated π -orbital system of the graphite and insertion of oxygen-containing functional groups into carbon base structure [14]. A chemical reduction of GO results in a lowering of the intensity of the functional groups peaks, thus suggesting the removal of oxygen-containing groups.

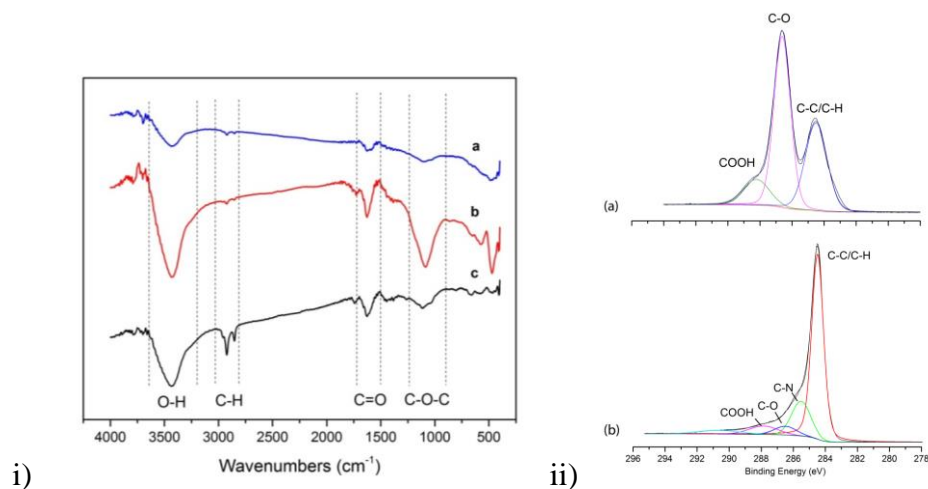


Figure 3. i) Spectra of fourier transformation infrared spectroscopy of (a) graphite, (b) GO and (c) rGO, ii) The C1s spectra of (a) GO and (b) rGO

XPS spectra of GO and rGO samples are presented in figure 3 (ii). The C1s XPS spectrum (Fig 3(ii)a) of GO reveal a definite degree of oxidation composed of three oxygen functional groups namely i) the carboxyl group (C(O)OH), ii) the C in C-O bonds and iii) non-oxygenated carbon (C-C). The carbon and oxygen content present on the specimen surface were calculated using the atomic sensitivity factors which showed an oxygen carbon level of 34% and 66% respectively. XPS spectrum of rGO displayed similar functional groups in the sample but with a reduced intensity peaks of oxygenated groups while the non-oxygenated carbon group displayed a relatively high intensity (Fig 3(ii)b). An added C-N peak in rGO spectrum is based on the fact that the chemical reduction of GO took place in the environment of hydrazine hydrate having nitrogen as a key element. The percentages of oxygen and carbon on the specimen surface came out to be 10% and 90%.

SEM analysis (Fig 4) reveals the difference between the surfaces of bare GF and coated GF covered with graphene nanosheets. The coating being uniform suggests that graphene can be deposited over the fiber surface electrophoretically which can be controlled by varying the deposition parameters [15].

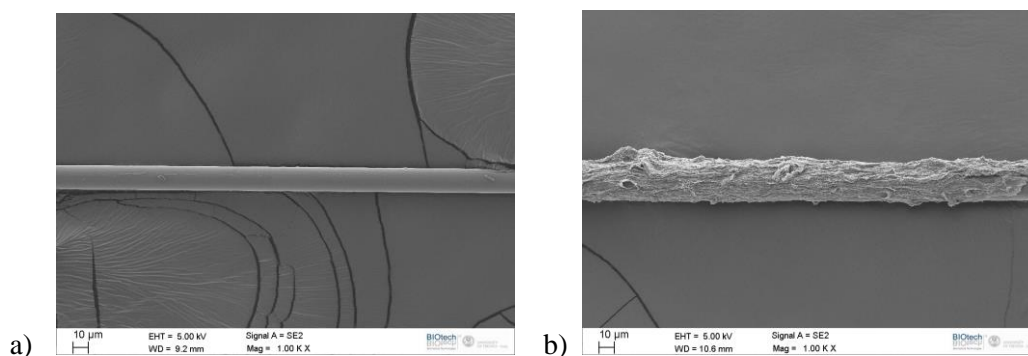


Figure 4. Scanning electron microscopy image of a) bare GF and b) GF coated with GO nanosheets at 10V/cm through electrophoretic deposition

Electrical conductivity of three different composites were tested. In case of clean epoxy composites reinforced by uncoated glass fibers (GF/Ep), the volume resistivity was measured to be in the range of $10^{14} \Omega \text{ cm}$ which is obvious since there is no conductive path in the composite for electron mobility. In the second case, the GF were coated with GO through EPD process and its composite with epoxy (GF/GO/Ep) also didn't show any enhancement in volume resistivity as compared to clean composite which came out to be in the range of $10^{13} \Omega \text{ cm}$, because of insulating nature of GO [16]. However, for the composite having rGO interphase (GF/rGO/Ep), the composite showed a very low volume resistivity of $10^2 \Omega \text{ cm}$. The remarkable drop in resistivity thus confirms the reduction of GO and hence making the graphene sheets conductive.

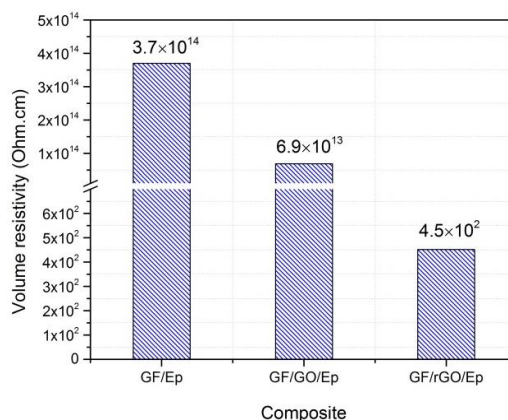


Figure 5. Volume resistivity of various composites (GF/Ep: composite without any deposited interphase, GF/GO/Ep: composite with GO deposited as interphase, GF/rGO/Ep: composite with rGO deposited as interphase)

The piezoresistive response of GF/rGO/Ep composites was assessed using electrical resistance change method. This method involves subjecting composites to mechanical loading and simultaneously measuring the absolute resistance through electrometer by two point method. In case of tensile loading (Fig. 6), it is interesting to observe that the electrical resistance decreased within initial 0.1% applied strain (Fig. 6b), which could be attributed to the rearrangement of the coated fibers at the microscale level thus promoting better electrical coupling among each other therefore the observed decrease in resistance. As the applied strain increased (Fig 6a), the change in resistance increased progressively till it became steep after 0.2% applied tensile strain. Considering this, a tangent line in this elastic portion provided a gage factor of ~ 11 according to the formula ($k = (\Delta R/R_0)/\epsilon$). Since the Poisson's ratio of the composite analyzed was 0.36, the factor ($\Delta\rho/\rho_0$) appeared to be approximately 0.01. In the plot 7a, an illustration of the piezoresistivity of the specimen's base portion which experienced tensile stress during flexural loading is shown. Here the understanding of resistance change can be easily observed by considering the influence of stresses acting on the fibers. Till 2.5% of flexural strain, the resistance change was steady until the fibers started to break resulting in failing of the specimen which consequently had an intense effect on the relative change of resistance. Similar behavior can be also visualized from the information gathered when the compressive stress zone of the specimen was monitored for piezoresistivity. First 0.5% flexural strain showed a decrease in electrical resistance however the rest of the strain had resulted in continuous increase in electrical resistance change hence confirming the strain sensing behavior of the hybrid composites. The observation of decreasing resistance was also noted in both cases here which is elaborated in figs. 7b and 7d which was previously reported above in case of tensile loading (Fig 6).

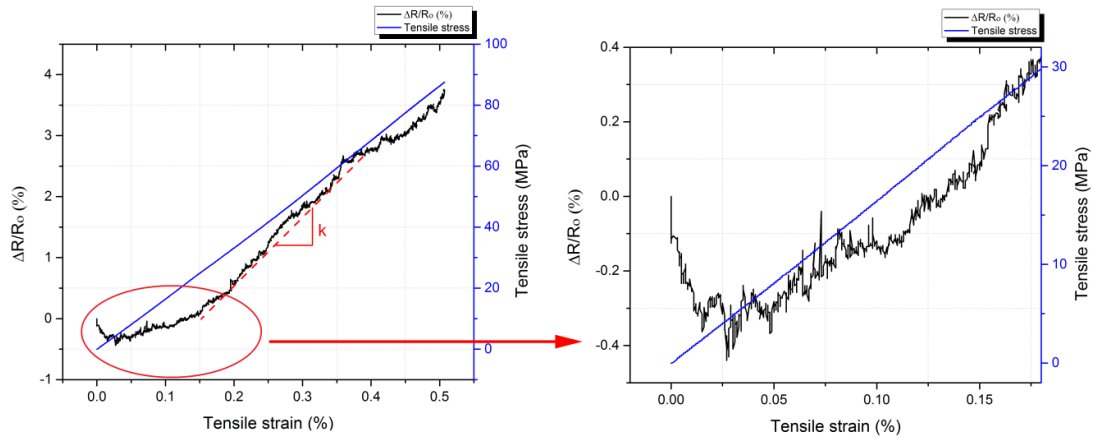


Figure 6. Piezoresistivity of GF/rGO/Ep composites - tensile loading condition

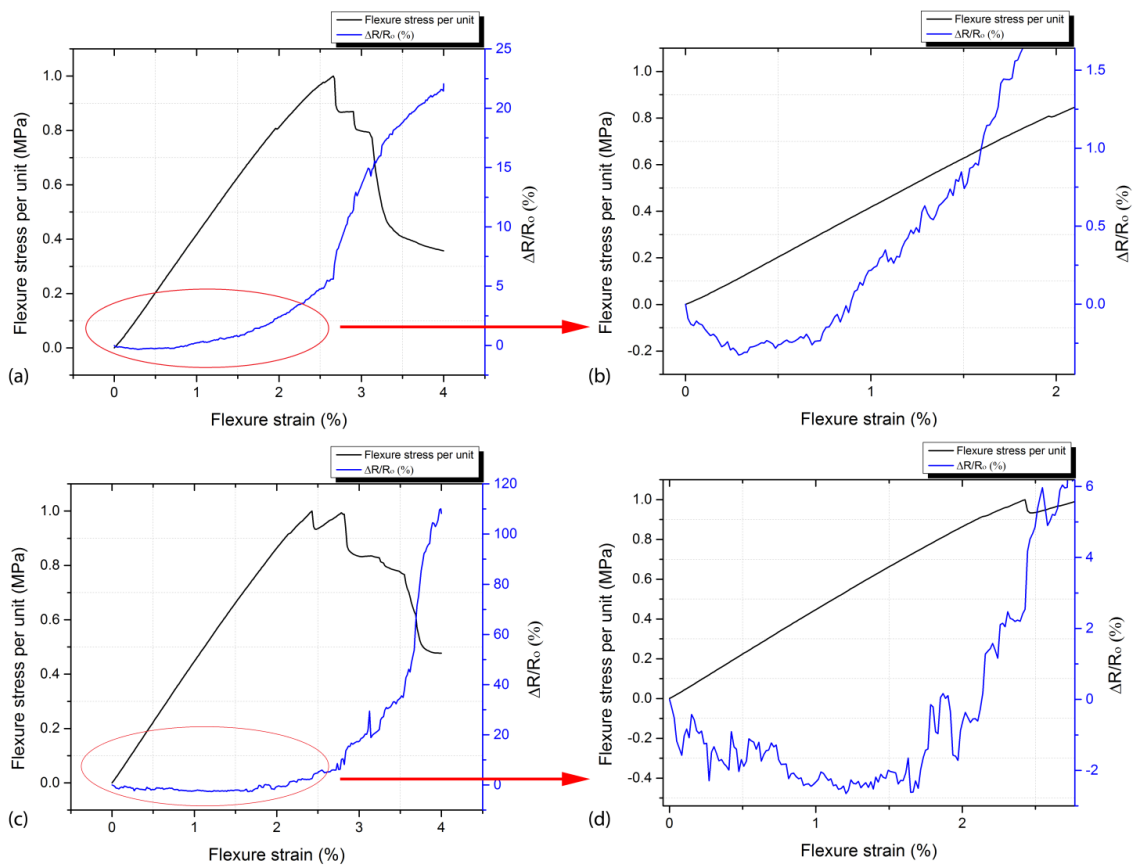


Figure 7. Piezoresistivity of GF/rGO/Ep composites under flexural loading with electrodes on: a & b) tensile subjected side (normal and magnified view), c & d) compression subjected side (normal and magnified view)

The reversibility of electrical network was tested by applying repeated loading-unloading condition. At least 50 cycles in the strain range $0.1\% < \epsilon < 0.5\%$ were applied and resistance was measured during each applied loading and unloading part of the cycle. Figure 8a demonstrates the piezoresistivity in cyclic conditions in which the average value of electrical resistance decreases by about 21% in the first

ten cycles then reaching a quite stationary level. Moreover, it is interesting to observe that the overall trend of the cycles of electrical resistance change is diminishing during the first 17 cycles afterward it almost levels out. This particular behavior could be related to the initial remark in Figs. 6-7 in which the decrease of resistance was observed under initial loading part. The same assumption can be applied here that during these first 17 cycles, the electrical contacts between the conductive fibers are improving in the insulating matrix of epoxy hence why the resistance is overall decreasing of the specimen together. By looking the last 10 cycles closely (Fig. 8b), the reversible piezoresistivity of the investigated materials can be confirmed. The gage factor and the factor ($\Delta\rho/\rho_0$) calculated here were ~ 3.8 and ~ 0.006 respectively in the case of these last cycles.

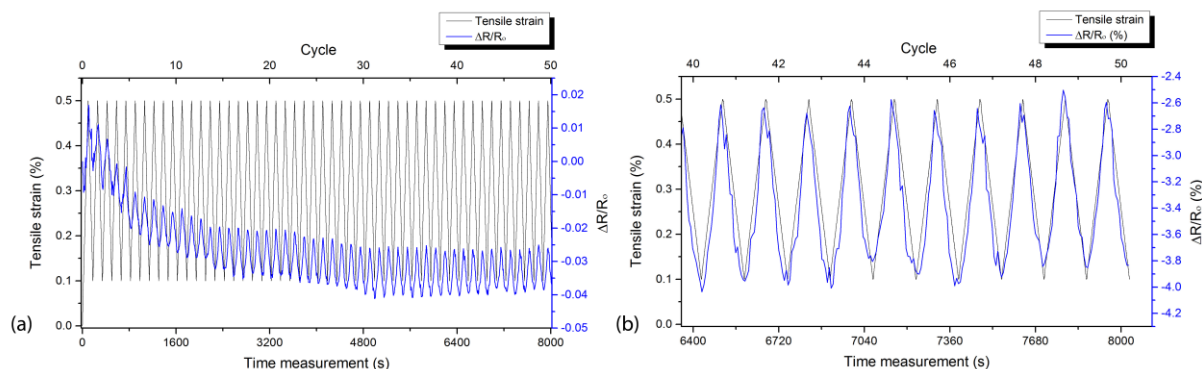


Figure 8. Piezoresistivity of the samples in reversible mode (a) 50 strain cycles under tensile loading and (b) detail of the last 10 cycles.

4. Conclusions

Hybrid epoxy composites with deposited rGO interphase on GF showed reversible piezoresistivity phenomenon when mechanical strain under various loading conditions are applied. The deposited rGO on GF showed a fair amount of uniformity of coating. This interphase created conductive pathway for electron mobility hence confirming the reduction of GO and making the composites on the whole conductive in nature. This reduction was also confirmed through different characterization techniques thus proving the lower amount of functional groups attached and the consequent depression of the oxygen content. Upon applying strain on the composite in different mechanical modes, the piezoresistivity was confirmed by the variation of absolute resistance. Moreover, an interesting behavior of lowering of resistance while initial part of loading was observed which is attributed to the improvement of electrical network of the fibers while loading. Overall, the resistance change while applied strain confirms the applicability of composites having hybrid interphase for strain monitoring application.

References

- [1] D. Pedrazzoli, A. Pegoretti, and K. Kalaitzidou, Interfacial interactions in silica-reinforced polypropylene nanocomposites and their impact on the mechanical properties, *Polymer Composites*: n/a-n/a, 2015.
- [2] H. Mahmood, M. Tripathi, N. Pugno, and A. Pegoretti, Enhancement of interfacial adhesion in glass fiber/epoxy composites by electrophoretic deposition of graphene oxide on glass fibers, *Composites Science and Technology*, 126: 149-157, 2016.

- [3] A. Rasheed and F. A. Khalid, Fabrication and properties of CNTs reinforced polymeric matrix nanocomposites for sports applications, *IOP Conference Series: Materials Science and Engineering*, 60, p. 012009, 2014.
- [4] X. Sun, H. Sun, H. Li, and H. Peng, Developing Polymer Composite Materials: Carbon Nanotubes or Graphene?, *Advanced Materials*, 25: 5153-5176, 2013.
- [5] L. Böger, M. H. G. Wichmann, L. O. Meyer, and K. Schulte, Load and health monitoring in glass fibre reinforced composites with an electrically conductive nanocomposite epoxy matrix, *Composites Science and Technology*, 68: 1886-1894, 2008.
- [6] A. C. Ferrari, F. Bonaccorso, V. Fal'ko, K. S. Novoselov, S. Roche, P. Boggild, *et al.*, Science and technology roadmap for graphene, related two-dimensional crystals, and hybrid systems, *Nanoscale*, 7: 4598-4810, 2015.
- [7] K. S. Novoselov, A. K. Geim, S. V. Morozov, D. Jiang, Y. Zhang, S. V. Dubonos, *et al.*, Electric field effect in atomically thin carbon films, *Science*, 306: 666-9, 2004.
- [8] C. Lee, X. Wei, J. W. Kysar, and J. Hone, Measurement of the Elastic Properties and Intrinsic Strength of Monolayer Graphene, *Science*, 321: 385-388, 2008.
- [9] K. S. Hu, D. D. Kulkarni, I. Choi, and V. V. Tsukruk, Graphene-polymer nanocomposites for structural and functional applications, *Progress in Polymer Science*, 39: 1934-1972, 2014.
- [10] J. Chen, D. Zhao, X. Jin, C. Wang, D. Wang, and H. Ge, Modifying glass fibers with graphene oxide: Towards high-performance polymer composites, *Composites Science and Technology*, 97: 41-45, 2014.
- [11] W. S. Hummers and R. E. Offeman, Preparation of Graphitic Oxide, *Journal of the American Chemical Society*, 80: 1339-1339, 1958.
- [12] S. Watcharotone, D. A. Dikin, S. Stankovich, R. Piner, I. Jung, G. H. B. Dommett, *et al.*, Graphene-Silica Composite Thin Films as Transparent Conductors, *Nano Letters*, 7: 1888-1892, 2007.
- [13] A. Buchsteiner, A. Lerf, and J. Pieper, Water Dynamics in Graphite Oxide Investigated with Neutron Scattering, *The Journal of Physical Chemistry B*, 110: 22328-22338, 2006.
- [14] P. Lian, X. Zhu, S. Liang, Z. Li, W. Yang, and H. Wang, Large reversible capacity of high quality graphene sheets as an anode material for lithium-ion batteries, *Electrochimica Acta*, 55: 3909-3914, 2010.
- [15] A. Chavez-Valdez, M. S. P. Shaffer, and A. R. Boccaccini, Applications of Graphene Electrophoretic Deposition. A Review, *The Journal of Physical Chemistry B*, 117: 1502-1515, 2012.
- [16] S. Rao, J. Upadhyay, and R. Das, "8 - Manufacturing and characterization of multifunctional polymer-reduced graphene oxide nanocomposites A2 - Dong, Yu," in *Fillers and Reinforcements for Advanced Nanocomposites*, R. Umer and A. K.-T. Lau, Eds., ed: Woodhead Publishing, 2015.